I&EC research
Industrial & Engineering Chemistry Research
pubs.acs.org/IECR
Review

Biomass-Derived Carbon for Electrode Fabrication in Microbial Fuel Cells: A Review

Wei Yang* and Shaowei Chen*

Cite This: *Ind. Eng. Chem. Res.* 2020, 59, 6391−6404

ABSTRACT: Natural biomass is a promising candidate for the preparation of heteroatom-doped carbons that can be used as effective electrode catalysts for microbial fuel cells (MFCs), due to its intriguing features, such as high abundance, rich heteroatom contents, and low cost. In this review, we summarize recent process in the design and fabrication of MFC electrodes based on biocarbons; discuss the effects of preparation methods, bacteria/electrode interaction, pore structure, and assembly procedure on the electrode and cell performance; and conclude with a perspective highlighting the strategies and critical challenges in electrode fabrication for further enhancement of the device performance.

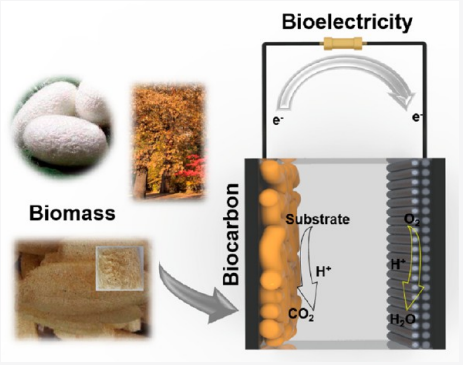

1. INTRODUCTION

Over the past few decades, the energy crisis and environmental pollution have become two major global issues.[1−3] Development of renewable technologies for energy conversion and environmental protection has been attracting extensive interest. Of these, the microbial fuel cell (MFC) is a device that can use anode microbes to catalyze the degradation of organic matter in wastewater and achieve power production simultaneously, holding a potential to alleviate or even eliminate these issues.[4−7] Of the various types of MFCs, the air cathode MFC has been regarded as a highly feasible technology for practical application, due to its simple structure and air-breathing design.[8,9] Nevertheless, despite substantial progresses, low power output and high costs remain the main bottlenecks for the widespread application of MFCs.

Electrodes are the key components that determine the fabrication cost and performance of air-cathode MFCs. In principle, the MFC power output depends mainly on the rate of substrate oxidation at the anode and the oxygen reduction reaction (ORR) at the cathode. As such, a range of factors have been found to significantly impact the MFC performance, such as extracellular electron transfer, microbial attachment and biofilm growth, ORR kinetics, and oxygen/substrate and ion diffusion[10−14] that are usually related to the properties of the electrode materials. The physical and chemical properties vary for different electrode materials (e.g., biocompatibility, specific surface area, pore structure, surface functionality, electrical conductivity, and chemical stability), which affect the microbial attachment, biofilm growth and extracellular electron transfer on the anode, and oxygen diffusion and ORR kinetics on the cathode. Therefore, development of effective electrode materials is of great significance to achieve high cell performance and promote the practical application of MFCs.

A wide variety of electrode materials have been examined in the last few decades.[15,16] Precious metals such as gold have been used as electrode materials in MFCs, due to their high electrical conductivity, unique mechanical strength, and high biocompatibility. To reduce the costs of electrode fabrication, transition metals, such as stainless steel, nickel, aluminum, titanium, and copper, have also been used.[17−23] However, these metals, especially when passivated before use, are not feasible for microbial growth and biofilm formation. Therefore, additional surface modification is necessary to improve biocompatibility and to facilitate electron transfer.[24] Recently, carbon-based materials, such as graphene and carbon nanotubes, have been attracting extensive attention for electrode fabrication because of their satisfactory conductivity, excellent microbial adhesion, high specific surface area, and pore structure.[25−32] Many studies have shown that carbon-based anodes can significantly promote microbial colonization and biofilm formation and hence enhance the extracellular electron transfer and anode reaction rate.[33−36] In addition, with the incorporation of select heteroatoms, the carbon-based materials also exhibit an apparent catalytic activity toward ORR. However, it should be noted that the energy density in

Received: January 2, 2020
Revised: March 9, 2020
Accepted: March 16, 2020
Published: March 16, 2020

https://dx.doi.org/10.1021/acs.iecr.0c00041
Ind. Eng. Chem. Res. 2020, 59, 6391−6404

wastewater is usually 3 orders of magnitude lower than conventional fuels, such as methanol, formic acid, and hydrogen, and the power output of MFCs is at least 2−3 orders of magnitude lower than those of a direct methanol fuel cell, a direct formic acid fuel cell, and a hydrogen−oxygen fuel cell.[37−42] Although with an apparent ORR activity, the use of graphene and carbon nanotubes for bulk electrode fabrication is still rather expensive for MFCs because the preparation of these carbon nanomaterials involves expensive and sophisticated equipment with high running costs and long production times. Furthermore, to facilitate the ORR activity of nanocarbons, additional costs are necessary for heteroatom doping using expensive chemical reagents.

Alternatively, carbon materials derived from biomass for electrode preparation can be a low-cost and sustainable approach. Recent studies have shown that biomass-derived carbon consists of an ordered and interconnected macroporous structure, which can facilitate the diffusion of electrolyte ions in the anode as well as the growth and immobilization of microbes.[43−45] Furthermore, due to the doping of natural heteroatoms and structural defects, the biomass-derived carbon exhibits an apparent ORR activity, and its performance can even rival that of state-of-the art Pt-based catalysts. Biomass-derived carbon can thus serve as a viable electrode material for MFCs.

In this review, we first summarize recent progress in biomass-derived carbon electrodes (both anodes and cathodes) for MFCs; discuss their fabrication, modification, and performance; and conclude with a perspective highlighting the strategies and challenges in electrode fabrication that plays a critical role in device optimization.

2. BIOMASS-DERIVED CARBON ANODE

2.1. Preparation Methods. Plants are the most commonly used natural precursors for the preparation of carbon anodes. The carbon in green plants is from the fixation of carbon dioxide by photosynthesis, while the heteroatom contents are closely related with the enzymes that participate in the photosynthesis under sun light.[46] Porous carbons are usually obtained by direct pyrolysis at high temperatures of these green precursors. During the preparation, heteroatoms in the plants serve as natural dopants, resulting in self-doped carbon, whereas the evaporation of water during the high-temperature pyrolysis leads to the formation of a porous carbon structure. For example, Zhang et al.[43] prepared three-dimensional (3D) microporous, N-, P-, and S-self-doped carbon foams (NPS-CFs) as free-standing anodes in MFCs by direct pyrolysis of commercial bread, which exhibited abundant pores and a large specific surface area (295.07 m^2/g), a good distribution of N, P, and S dopants, and excellent electrical conductivity (Figure 1). An MFC equipped with an NPS-CF anode delivered a maximum power density of 3134 mW/m^2 and current density of 7.56 A/m^2, which is approximately 2.5 times that with a carbon cloth anode (1218 mW/m^2 and 2.87 A/m^2).

As summarized in Table S1, a large number of natural materials have been used for the fabrication of MFC anodes, where the surface properties, accessible surface area, and pore structure are the dominating factors that impact the device performance and should be considered during anode preparation. For example, Chen et al.[47] fabricated a hierarchically structured anode using chestnut shells as a precursor due to its brush-like structure with dense and hard thorns stretching out on the spherical shell, which can provide an extended accessible surface for biofilm formation. The as-prepared anode achieved a maximum power density of 759 ± 38 mW/m^2 and Coulombic efficiency of 75 ± 12%, which are comparable to those of a traditional graphite brush anode (Figure 2a−c). In another study, it is also found that the chestnut shell-derived anode, after chemical activation, delivered a maximum power density of 23.6 W/m^3, 2.3 times higher than that with a carbon cloth anode (10.4 W/m^3).[44] To increase the active bacterial loading with no increase in the volume and weight of the anode, Zhu et al.[48] prepared hollow structure fibers as the anode material, where both the outside and inside surfaces were accessible for electron transfer. In fact, the weight-based power density of the anode (104.1 mW/g) was about 20 times higher than that of a traditional solid carbon fiber electrode (5.5 mW/g) (Figure 2d−f).

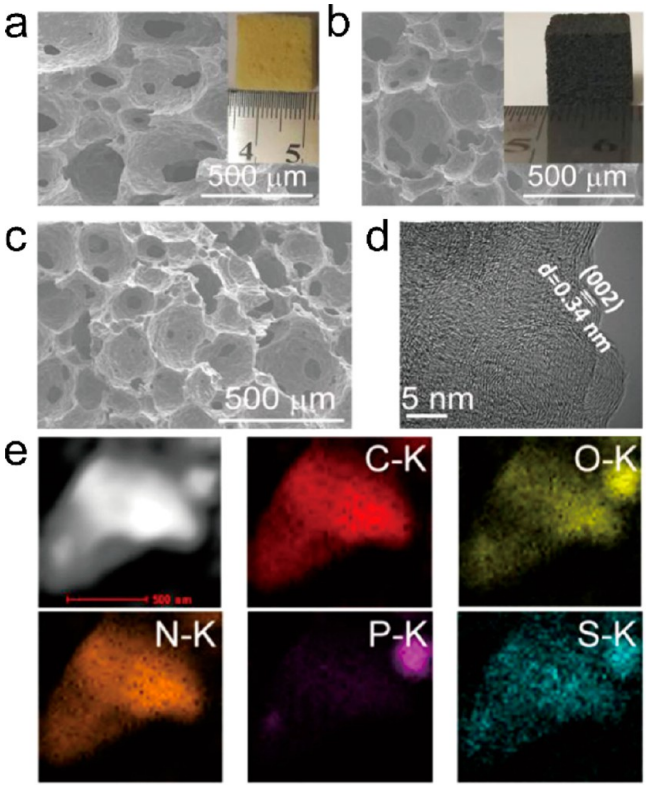

Figure 1. SEM of bread (a) before and (b, c) after pyrolysis at 1000 °C. (a, b) Top view images and (c) cross-sectional view. Insets are the corresponding photographs of the bread. (d) HRTEM image and (e) STEM−EDS mapping images of C, N, O, P, and S of NPS-CF-1000. Reprinted with permission from ref 43. Copyright 2018, Elsevier.

In addition to the pyrolysis pathway, simple coating of the natural precursors with conductive carbon nanoparticles is an energy-saving approach to anode preparation. For example, Xie et al.[49] synthesized a carbon nanotube (CNT)−textile anode by dipping-drying of a piece of textile in aqueous CNT ink; the as-synthesized anode delivered a 157% higher maximum current density and 68% higher maximum power density than traditional carbon cloth anode. Zhou et al.[50] prepared a 3D anode by soaking a natural loofah sponge with Chinese ink, which exhibited remarkable flexibility and an open porous structure. The anode also showed satisfactory stability over an experimental period of more than 70 d, and a high current density of 16.3 ± 0.5 mA/cm^3, close to that of a 3D electrode produced by the carbonization process (Figure 2g−i). In a similar study, Zhang et al.[51] observed a maximum power

https://dx.doi.org/10.1021/acs.iecr.0c00041
Ind. Eng. Chem. Res. 2020, 59, 6391−6404

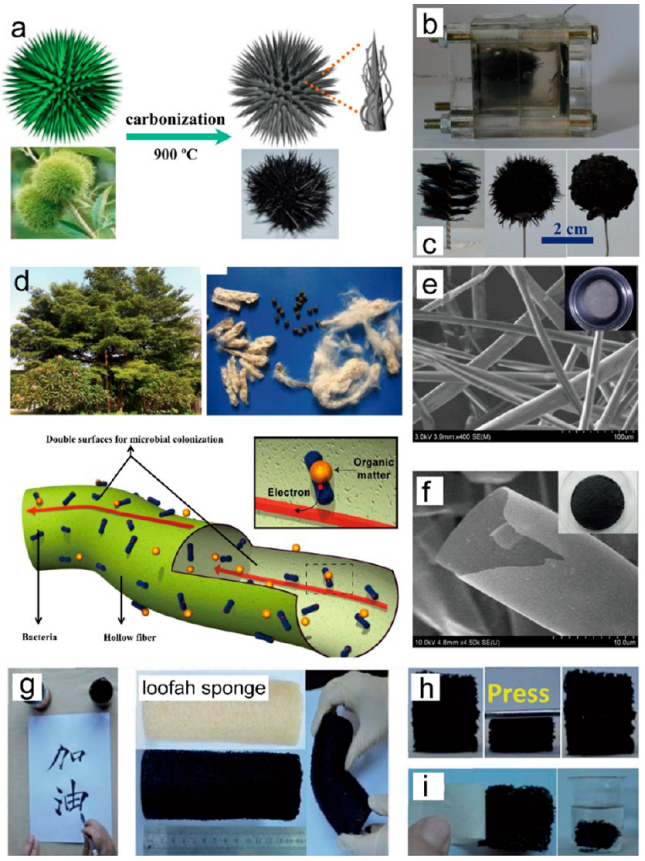

Figure 2. (a) Schematic illustration of the preparation of a chestnut shell anode. (b) Photograph of an MFC equipped with the chestnut shell anode. (c) Photographs of the graphite brush and chestnut shell anode. Panels (a–c) reprinted with permission from ref 47. Copyright 2016 Elsevier. (d) Photographs and schematic of a hollow kapok fiber anode. SEM images of the kapok fiber (e) before and (f) after carbonization. Insets are the photographs of the corresponding samples. Panels (d–f) reprinted with permission from ref 48. Copyright 2014 Elsevier. (g) Photographs of a loofah sponge before (white) and after (black) ink coating. (h) The recovery process of a compressed loofah sponge anode, and (i) evaluation of the durability of the loofah sponge anode by performing a Scotch tape test and soaking in water. Panels (g–i) reprinted with permission from ref 50. Copyright 2016 Royal Society of Chemistry.

density of 61.7 ± 0.6 W/m^3 with an MFC based on a carbon back-loaded loofah sponge anode. This suggests that the soaking method can serve as a generic, low-cost route for anode fabrication.

In summary, direct pyrolysis of biomass precursors at high temperatures is the most commonly used method for anode preparation, by which the biomass can be transformed into porous carbon with the self-incorporation of heteroatoms. However, intensive energy input in the pyrolysis process inevitably increases the preparation cost of anodes. Alternatively, coating conductive carbon nanoparticles onto the natural precursors is a promising, low-cost, and simple procedure for anode preparation.

Apart from plants, other types of biomass from animals and sewage sludge have also been used as precursors for MFC anode preparation. As one of the most abundant natural polymer composites, silk cocoon has a high nitrogen content (~15%) and an intrinsically 3D nonwoven structure with multiple layers and pores generally by random arrangement of one single silk fiber. These intriguing features make silk cocoon a suitable candidate for anode fabrication. For example, Lu et al.[52] prepared a freestanding and flexible bioanode with a rich nitrogen content and hierarchical pores by simple one-step carbonization of silk cocoon. The prepared flexible carbon fiber anode showed good mechanical strength and yielded a maximum gravimetric power density 3.1 times higher than that of a carbon cloth anode in MFCs (Figure 3). Different

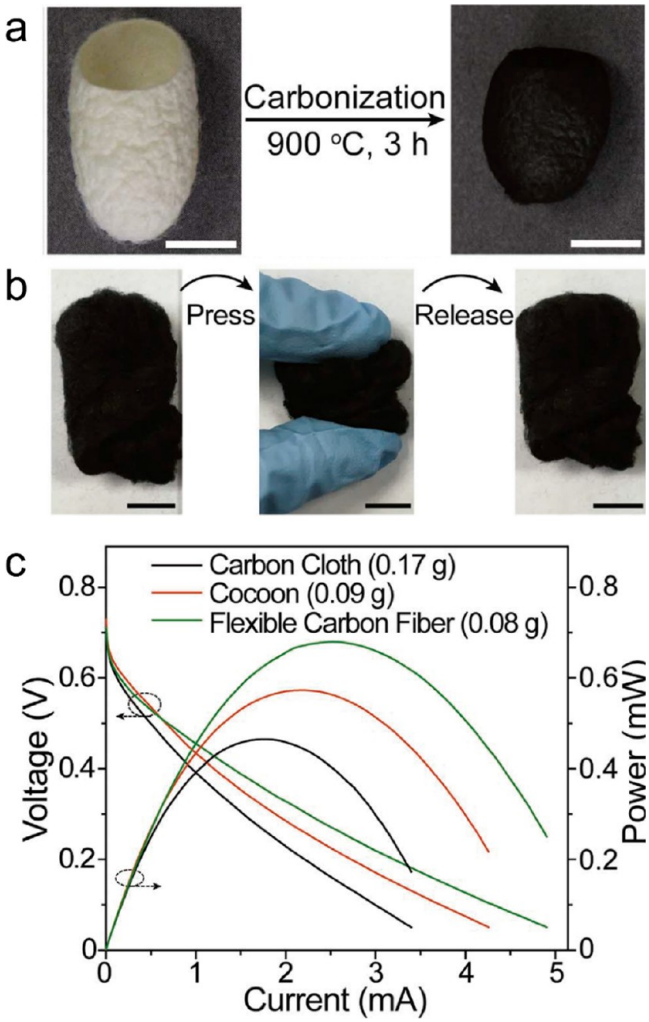

Figure 3. (a) Schematic of the carbonization of silk cocoon. (b) Digital photographs of the carbon fibers derived from silk cocoon in mechanical flexibility tests by finger-tip pressing. (c) Polarization curves and power curves of MFCs equipped with different anodes. Reprinted with permission from ref 52. Copyright 2016 Elsevier.

from silk cocoon, sewage sludge is the main byproduct of wastewater treatment and widely used as catalysts for chemical reactions due to its abundant surface functional groups and high carbon contents.[53,54] In fact, sewage sludge has also been used for anode fabrication. For example, Yuan et al.[55] prepared a carbon monolith anode by directly carbonizing sewage sludge at 900 °C and found that the anode delivered a maximum power density of 486 ± 18 mW/m^2, which was higher than that of a conventional graphite plate anode (410 ± 10 mW/m^2) in MFCs. It should be noticed that although with a large number of functional groups on the anode surface the pore sizes of the sewage sludge-derived carbon anodes are generally in the micrometer range; thus, clogging of pores can

https://dx.doi.org/10.1021/acs.iecr.0c00041
Ind. Eng. Chem. Res. 2020, 59, 6391–6404

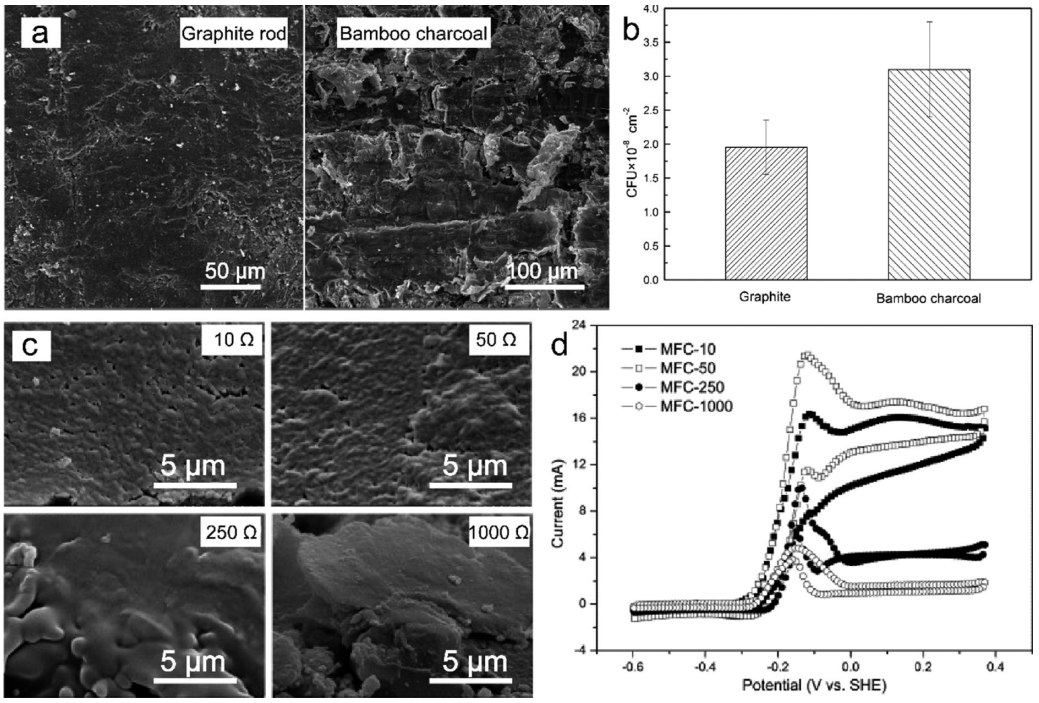

Figure 4. (a) SEM images and (b) microbial growth on graphite and bamboo charcoal tube surfaces. Panels (a, b) reprinted with permission from ref 62. Copyright 2014 Elsevier. (c) SEM cross-sectional images. (d) Cyclic voltammograms of the biofilm obtained at varied external resistances (10, 50, 250, and 1000 Ω). Panels (c, d) reprinted with permission from ref 63. Copyright 2011 Elsevier.

significantly limit the microbial colonization and volume utilization of the anode.

2.2. Bacteria–Surface Interaction. The interaction between bacteria and the anode surface can be reflected by the formation of a bacteria biofilm, as a result of the anode surface properties. In fact, studies of biofilm have been focused on various factors, such as formation dynamics, electron transfer, growth, and metabolic activity.[56,57] It is widely accepted that the development of biofilm usually involves multiple steps: (i) attachment of bacteria on the electrode surface, (ii) formation of monolayer and multilayer bacteria, (iii) formation of a polymeric scaffold, and finally, (iv) maturation of biofilm forming a 3D structure.[58] Among these, the attachment and formation of monolayer bacteria are the critical steps that determine the subsequent development of biofilm. Notably, the initial attachment and monolayer bacteria adhesion are highly regulated by the electrode surface properties, such as hydrophilicity/hydrophobicity, chemical functionality, and micro/nanotexture.[59] At this stage, the anode usually shows a poor electrocatalytic activity and a low current output due to the low bacteria density on the anode surface. However, after the maturation of biofilm, the viability and catalytic activity of biofilm can be significantly enhanced.

Chemical modification is an effective approach to alter the surface properties and facilitate bacteria attachment and electron transfer. In general, the anode can be modified with metal nanoparticles, polymers, or (electro)chemical treatment. Among these, (electro)chemical oxidation is a fast and cost-effective approach, whereby specific functional groups and morphologies are introduced onto the anode surface to facilitate bacteria attachment and charge transfer.[60] Interestingly, biomass-derived anodes usually have abundant functional groups due to the inherent heteroatom incorporation. For example, Wang et al.[61] prepared a free-standing anode by one-step carbonization of pinecone and found that the extracellular electron transfer rate and exoelectrogens attachment were related to the ratio of the N and P dopants on the anode surface. The anode prepared by pyrolysis at 900 °C had the highest N content and hence delivered the highest power density of 10.88 W/m^3, which was 2.20 times that of a carbon felt anode in MFCs.

The roughness of the electrode surface is another factor affecting the anode biofilm formation. Zhang et al.[62] prepared bamboo charcoal tubes as a novel anode substrate by carbonizing natural bamboo branches and observed that the tubular anode had a rougher surface with many obvious cracks than traditional graphite rod anodes, which provided a higher specific surface area and more attaching sites for biofilm formation. The as-prepared bamboo charcoal anode also displayed better biofilm growth, improved active bacteria attachment, and enhanced electron transfer from bacteria to the electrode, as compared to a traditional graphite rod anode (Figure 4a and b).

Biofilm regulation is generally employed to optimize biofilm maturation on the anode surface and hence improve mass transport within the biofilm. Since the current response of the anode is closely related with mass transport in the bacteria biofilm and electron transfer between the bacteria and electrode surface, the anode current response of the biofilm can be used as an external inducible factor to regulate the formation of maturation biofilm. For example, Zhang et al.[63] investigated the effect of external resistance (10, 50, 250, 1000 Ω to produce different current responses) on biofilm formation and observed that the anode operated at low resistances (i.e., 10 and 50 Ω, corresponding to a high current output) and produced extensive voids within the biofilm, which were conducive to mass transport of the substrate and buffer supply as well as product removal within the biofilm. However, excessive void spaces within the biofilms could also lead to imperfect contact between the bacteria and the anode surface

https://dx.doi.org/10.1021/acs.iecr.0c00041
Ind. Eng. Chem. Res. 2020, 59, 6391–6404

and hence a decrease in the electric conductivity of the biofilm and a decline of the anode performance. Consequently, the anode operated at 50 Ω was found to exhibit the best activity among the series of samples due to the optimal combination of void spaces in the biofilm and contact between the bacteria and the anode (Figure 4c). Similarly, Li et al.[64] studied the response of an anodic biofilm at different applied discharging current densities and observed that the anode biofilm cultivated at a higher current density induced more active bacteria attachment, better biofilm growth, and a higher electron transfer rate, as compared to those at lower current densities. However, an excessive current could also deteriorate the microenvironment of the biofilm and hence inhibit the biofilm formation.

2.3. Pore Structure. Anode porosity is another critical factor that affects the accessible surface area for microbial colonization and effective channels for mass transport. The size of bacteria cells usually ranges from 0.4 to 4 μm and mostly from 1 to 2 μm.[36,65,66] Several studies have shown that the pores from 2 to 10 μm can be used for internal colonization of bacteria cells. For example, Karthikeyan et al.[67] used carbonized plant materials as MFC anodes and found that anode derived from corn stem with pores ranging from 2 to 7 μm in diameter showed bacterial communities on both the external and internal surfaces (Figure 5a). However, the colonization of bacteria in the pores was limited by the pore size, and the thickness of the biofilms grown on the exterior surface was from 3 to 18 μm. It was then concluded that pores of approximately10 μm were enough to allow bacteria cells to easily penetrate into the pores, but as the biofilm continued to grow, clogging of the pores most probably occurred. Chen et al.[68] prepared a macroporous carbon anode derived from sponge-like natural product kenaf with pores tens of micrometers in diameter and found that the biofilm on the anode surface was more than 40 μm thick, but only few bacteria grew as deep as 100 μm into the pore structure of the electrode. Similarly, a porous anode prepared by carbonizing king mushrooms had pore sizes ranging from 10 to 120 μm, and parts of the pores were filled by biofilm after 18 d (Figure 5b).[67] Since mature biofilm can achieve a thickness of tens or hundreds of micrometers, porous electrodes with pore sizes around tens of micrometers are still insufficient for biofilm growth. Once the pores are clogged by the biofilm, the supply of substrate to and the removal of metabolites or ions from the interior of the electrode become impeded, which inhibits the growth of the biofilm and can cause death of the bacteria inside the pore structure.

Anodes with pore sizes around hundreds of micrometers have also been studied. It has been reported that anodes derived from wild mushroom with pore sizes ranging from 75 to 200 μm allow sufficient colonization of biofilm on the anode surface without clogging (Figure 5c).[67] This suggests that the pore sizes around hundreds of micrometers can effectively eliminate pore clogging by biofilm growth; nevertheless, colonization of bacteria inside pores needs to be further investigated. Chen et al.[69] fabricated a reticulated carbon foam anode with a pore size over 100 μm by carbonizing sponge-like natural product pomelo peel and observed that the biofilms could propagate inside the anode more than 600 μm in depth. The thickness of the biofilms near the anode surface was more than 15 μm and then decreased to 1.8 μm with the depth increased to 600 μm (Figure 5d–h). In this range of pore sizes, the porous anodes allow the penetration and colonization of

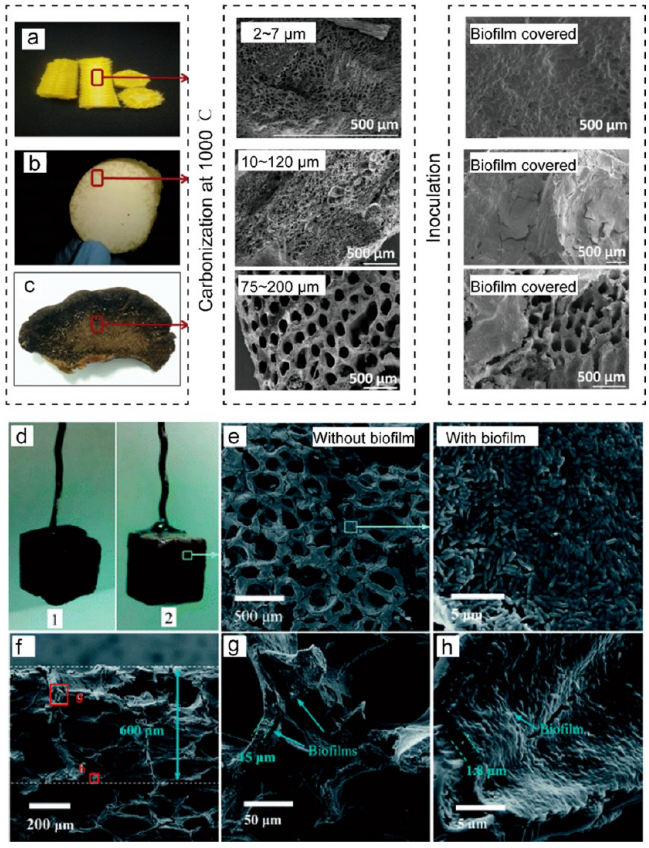

Figure 5. Digital photos and SEM images of carbon electrodes derived from (a) corn stem, (b) king mushroom, and (c) wild mushroom. Panels (a–c) adapted and reprinted with permission from ref 67. Copyright 2015 Elsevier. (d) Digital photos of reticulated carbon foam electrode (1) before and (2) after biofilm growth. (e) Top view and (f) cross-sectional view SEM images of biofilms on the surface of reticulated carbon foam electrode. (g, h) SEM images magnified at positions g and h in image f, respectively. Panels (d–h) adapted and reprinted with permission from ref 69. Copyright 2012 Royal Society of Chemistry.

bacteria on the internal structures, but the biofilm thickness is still apparently affected by the mass transport limitation, which impedes the growth of biofilm as the depth increases. Therefore, it is possible that only porous anodes with pore sizes of hundreds of micrometers or even up to the millimeter level will allow sufficient microbial colonization without a notable limiting effect. Chen et al.[70] prepared layered corrugated carbon anodes using corrugated cardboard as precursors and investigated the effect of anode flute heights (H = 1.4, 2.2, 2.9, and 3.2 mm, with length and width of 10 mm) on the current output. The results indicated that anodes with flute heights of 2.2 and 2.9 mm delivered a close but higher projected current density than others at 7.02 ± 0.52 and 7.28 ± 0.52 mA/cm^2, respectively. However, it should be noted that these anodes were usually operated and evaluated under the fed-batch mode, in which the electrolyte was almost stagnant. Significantly, anodes derived from biocarbons were also inoculated and operated under the continuous-flow mode. Flexer et al.[71] synthesized a monolithic anode with a hierarchical porous structure through hydrothermal carbonization of biomass-derived precursors. The results showed that the as-prepared anode exhibited a wide pore distribution with small pores from 1 to 3 μm and large pores from 10 to 50 μm,

https://dx.doi.org/10.1021/acs.iecr.0c00041
Ind. Eng. Chem. Res. 2020, 59, 6391–6404

and the pores and surface of the anode was fully clogged and covered by a thick and continuous biofilm. Li et al.[72] also evaluated the performance of bamboo charcoal tube anodes of four different inner diameters (1, 1.5, 2, and 3 mm) and found that the inner surfaces of all four anodes were covered by biofilms, and the mass transport resistance decreased with an increasing inner diameter. The anode with a diameter of 2 mm had the highest volumetric power density among the series, based on the volume of the MFC anode, revealing a suitable anode structure for the practical application of MFCs. It can be found that in both fed-batch and continuous-flow modes an anode with pore sizes from hundreds of micrometers to several millimeters may be the suitable structures for microbial colonization without biofilm clogging or growth inhibition of microbial cells.

In fact, bacteria growth in the pores of an anode can be affected by multiple factors, such as pore sizes, surface properties, bacterial culture temperature, and substrate concentration. It is therefore difficult to establish a direct, quantitative relationship between bacteria colonization and pore size. However, from the above analyses, we can observe an apparent trend: Pore sizes of several micrometers allow bacteria penetration, but the colonization of bacteria in the pores is limited by the pore size. With pore size in the range of tens of micrometers to approximately 100 μm, the biofilms can propagate inside the anode, but the thicknesses of the biofilms decrease as the depth increases, as limited by mass transport. With pore size in the range of hundreds of micrometers to millimeters, bacteria colonization is generally observed inside the pore structures without an obvious limiting effect.

It should be noted that the role of nanopores, such as micropores (<2 nm) and mesopores (2−50 nm), which dominate the specific surface area of the electrode, remains unrevealed. Actually, for pores in this size range, the interior is not suitable for bacteria colonization. Several studies have reported the role of nanopore structures in bioelectrochemical systems. For example, He et al.[73] synthesized a hierarchically porous chitosan/vacuum-stripped graphene scaffold as a bioanode and found that the nanopores in the anode could provide a huge internal surface area for endogenous mediators and thus improve electron transfer between bacteria and the anode. The as-prepared anode delivered a power density of 1530 mW/m^2, which was 78 times higher than that of a carbon cloth anode. Similar studies by Chen et al.[68] and Chen et al.[69] also highlighted the role of nanopores as active sites to trap the endogenous mediators for electron transfer. Apparently, these results can also be transplanted to the anode derived from the biomass. A quick comparison shows that thanks to the inherent heteroatom dopants and abundant functional groups, biomass-derived anodes can initiate bacteria attachment and colonization. However, as the pore structure of the biomass-derived anode is dictated mainly by the raw precursors, other interventions such as chemical activation are usually needed to regulate the pore distribution during anode fabrication.

3. BIOMASS-DERIVED CARBON CATHODE

3.1. Biomass Precursors of Cathode Catalysts. It is widely accepted that platinum and its alloys are the most active catalysts toward ORR, but their high costs and low poison resistance hinder their commercialization in MFCs. Natural biomass can serve as a promising precursor to prepare heteroatom-doped carbon as viable alternatives. The leading preparation strategies are summarized below.

Plant-derived biomass, frequently used precursors for ORR catalysts, are rich in N and P elements and can be used as a single precursor for both carbon and heteroatoms. Due to the inherent incorporation of heteroatoms and inexpensive raw precursors, the preparation of plant-derived cathode materials can eliminate the need of complicated reaction processes, specialized precursors and equipment, and multiple hazardous chemicals. For example, Zhong et al.[74] synthesized N-doped hierarchically porous carbon using watermelon rind as a N-rich and highly stable precursor and observed that the as-prepared sample exhibited a redox peak at the current density of 0.19 mA/cm^2 that was comparable to that of Pt/C but with a lower charge transfer resistance (20.63 Ω) than that (37.56 Ω) for Pt/C. Also, Fan et al.[75] prepared a high-performance ORR catalyst by directly pyrolyzing *Chlorella pyrenoidosa* at 900 °C and found that the MFC using the as-prepared catalyst delivered a maximum power density of 2068 ± 30 mW/m^2, which was 13% higher than that using 20 wt % Pt/C at the same loading.

Similar to anode fabrication, biomass from animals and sewage sludge has also been used to prepare carbonaceous cathode catalysts, primarily due to their rich N contents. By simple pyrolysis, N is incorporated into the porous carbon structure. For example, Yuan et al.[76] used spider silk to prepare carbon nanofibers as a sustainable electrocatalyst via a simple pyrolysis method, and the as-prepared catalyst delivered a power density of 1800 ± 82 mW/m^2 at the loading of 2 mg/cm^2, significantly higher than that of Pt/C (704 mW/m^2, 0.5 mg/cm^2) in MFCs. Furthermore, the as-prepared catalyst exhibited a stable output of the maximum power density during prolonged operation for up to 90 d (Figure 6). In an additional study from the group, N-doped carbon sheets were derived from chitin via a two-step procedure involving hydrothermal treatment and pyrolysis.[77] The obtained catalyst

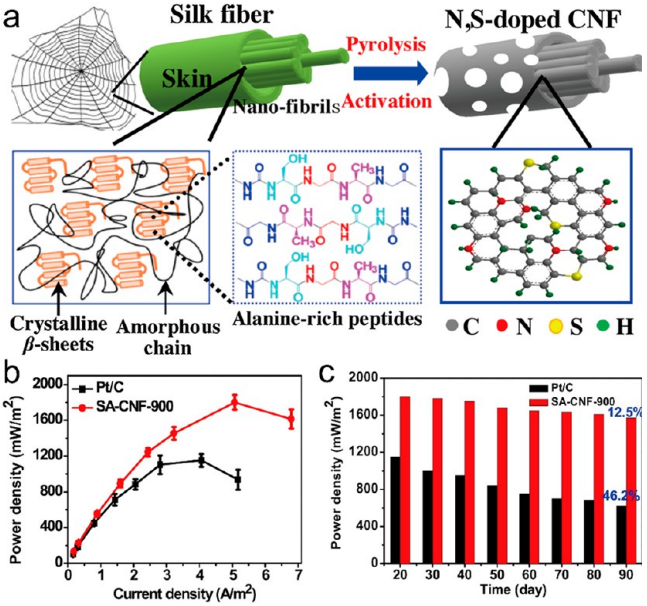

Figure 6. (a) Schematic of the preparation procedure of spider silk-derived carbon nanofibers (SA-CNF). (b) Polarization curves of MFCs with SA-CNF-900 and Pt/C as the cathode catalyst. (c) Maximum power densities of the MFCs with SA-CNF-900 and Pt/C as the cathode catalyst in continuous operation for up to 90 d. Reprinted with permission from ref 76. Copyright 2016 Elsevier.

https://dx.doi.org/10.1021/acs.iecr.0c00041
Ind. Eng. Chem. Res. 2020, 59, 6391−6404

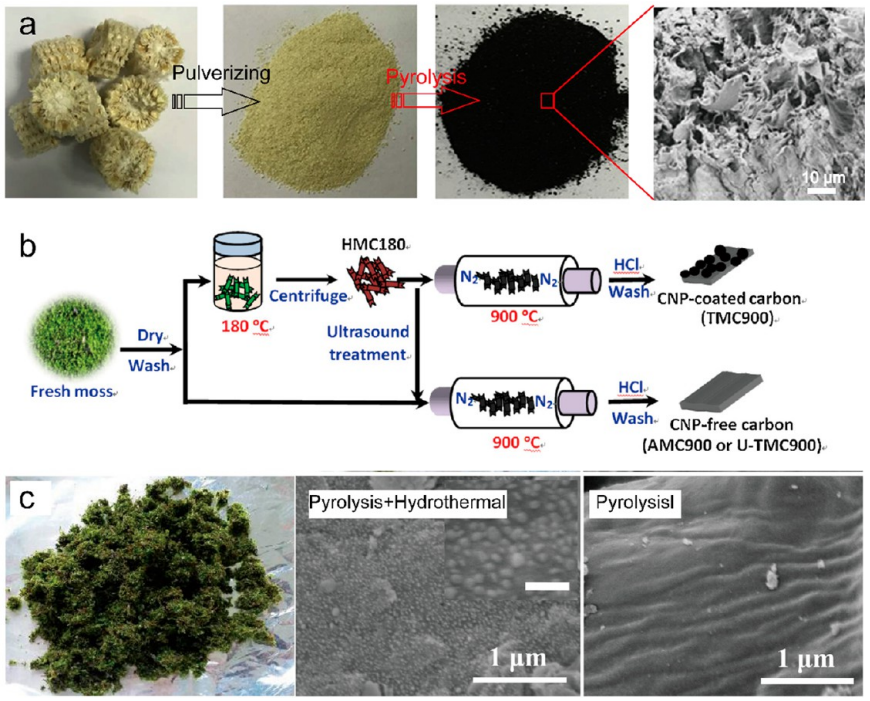

Figure 7. (a) Procedure for the preparation of porous carbon from corncob. Reprinted with permission from ref 79. Copyright 2018 Elsevier. (b) Procedure for the preparation of carbon from moss. (c) Photograph of moss plant and SEM images of carbon prepared with and without a hydrothermal process. Panels (b, c) reprinted with permission from ref 81. Copyright 2016 Elsevier.

had an onset potential (−0.15 V vs SCE) close to that of Pt/C (−0.13 V vs SCE) in alkaline media and achieved a maximum power density (705 ± 5 mW/m^2) that was comparable to that of Pt/C (727 ± 5 mW/m^2) in MFCs.

Apart from animal-derived biomass, the utilization of sewage sludge as cathode catalysts is a sustainable and waste recycling strategy. Deng et al.[78] prepared biocarbon from livestock sewage sludge, which, after KOH activation, exhibited a high ORR activity with a half-wave potential ($E_{1/2}$ = −0.07 V vs SCE) close to that of Pt/C (−0.04 V vs SCE) in a phosphate buffer solution. They found that the as-prepared carbon catalyst delivered a maximum power density (1273 ± 3 mW/m^2) similar to that of Pt/C (1294 ± 2 mW/m^2) and exhibited high stability after 3 months of operation (989 ± 4 mW/m^2 for as-prepared catalyst and 462 ± 5 mW/m^2 for Pt/C after 3 months). In these studies, the biocarbons derived from both natural plants, animals, and sewage sludge precursors all showed a satisfactory performance and stability in MFCs.

Significantly, it is found that most carbon derived from natural biomass is prepared by pyrolysis. During pyrolysis, thermochemical decomposition of organic matter occurs in the absence of water under an inert gas flow at high temperatures and usually does not involve reactions with oxygen, water, or other reagents.[46] For example, Li et al.[79] prepared a biocarbon using fresh corncob as a precursor, which was sun-dried for 5 days and then ground into powder. The powder was heated under a N_2 atmosphere between 250 and 750 °C for 2 h by a programmable furnace. The obtained catalysts exhibited a power density of 458.85 mW/m^2 in MFCs (Figure 7a). Besides pyrolysis, a hydrothermal procedure is also used in the catalyst preparation. During the hydrothermal process, biomass can be converted into carbon in an aqueous medium at moderate temperatures (typically 180 °C). For instance, Zhu et al.[80] reported a facile approach to synthesize carbon nanodots as electrocatalysts using soy milk as the raw precursor through a hydrothermal procedure at 180 °C for 3 h. During the hydrothermal process, carbon nanoparticles are produced as a result of carbonization of small organic molecules. However, the relatively low temperatures used in hydrothermal treatment typically lead only to a low degree of graphitization and hence poor electrical conductivity of the catalysts. A combination of hydrothermal treatment and pyrolysis can be exploited to mitigate these issues. For instance, Zhou et al.[81] prepared self-constructed, carbon nanoparticle-coated porous carbon derived from a natural plant moss (*Weisiopsis anomala*) through a hydrothermal treatment at 180 °C for 24 h, followed by carbonization at 900 °C under a N_2 atmosphere. They found that the hydrothermal process induced the formation of functional nanoparticles (i.e., carbon nanodots), which assembled on the porous carbon, leading to an increased specific surface area and enhanced accessibility of the active sites (Figure 7b and c). It was found that the as-prepared catalysts exhibited an $E_{1/2}$ of +0.832 V vs RHE in 0.1 M KOH and a power density of 703 ± 16 mW/m^2 in MFCs, which were obviously higher than +0.762 V and 494 ± 32 mW/m^2 for the sample prepared by direct carbonization alone.

3.2. Activation and Modification of Catalysts. It should be noted that heteroatom doping, specific surface area, and pore structure vary with biomass precursors, and the electrocatalytic activity of biomass-derived carbons may need to be further improved through activation or heteroatom incorporation during the synthesis to satisfy practical requirements. Various natural materials for the preparation of cathode catalysts are summarized in Table S2. It can be found that chemical activation and N- and P-doping are the widely used approaches. Chemical activation is a feasible method to expand the pore structure of the catalysts and increase the accessibility of ORR active sites. For example, Li et al.[82] reported a N- and

https://dx.doi.org/10.1021/acs.iecr.0c00041
Ind. Eng. Chem. Res. 2020, 59, 6391−6404

P-codoped carbon derived from onion by carbonizing the mixture of raw onion and KOH at 900 °C. The as-prepared catalyst exhibited a power density (742 ± 17 mW/m^2) comparable to that of Pt/C (763 ± 19 mW/m^2) in MFCs (Figure 8a). Similarly, Ye et al.[83] synthesized hierarchically

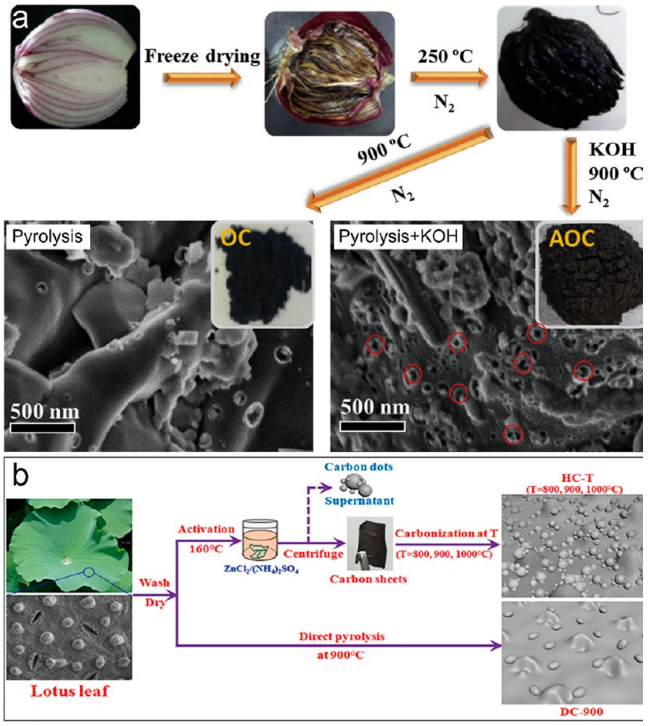

Figure 8. (a) Synthetic procedure and SEM images of the carbons derived from onion with and without KOH activation. Reprinted with permission from ref 82. Copyright 2017 Elsevier. (b) Carbon materials prepared from lotus leaves. Reprinted with permission from ref 83. Copyright 2019 Elsevier.

structured carbon derived from lotus leaves through the activation of $ZnCl_2$/$(NH_4)_2SO_4$, followed by carbonization at high temperatures. They found that the activation process significantly increased the specific surface area of the catalyst from 52.40 to 908.90 m^2/g, and the maximum power density (511.5 ± 25.6 mW/m^2) was markedly higher than that of Pt/C (486.7 ± 23.3 mW/m^2) in MFCs (Figure 8b). One can see that both KOH and $ZnCl_2$ activation can effectively increase the specific surface area and hence the activity of the catalysts. However, the study by Deng et al.[84] revealed that KOH activation could achieve a higher specific surface area (883.67 m^2/g) and catalytic activity (onset potential +0.21 V vs SCE) than $ZnCl_2$ activation (517.87 m^2/g and +0.18 V vs SCE) based on alfalfa leaf-derived carbon. The catalyst activated by KOH delivered a maximum power density of 1328.9 mW/m^2, significantly higher than that activated by $ZnCl_2$ (1099.3 mW/m^2).

Apart from chemical activation, heteroatom doping by the addition of select chemical compounds is a cost-effective approach to the improvement of the electrocatalytic activity of carbon materials. For example, Sun et al.[85] synthesized a cornstalk-derived N-doped carbon using melamine as an external nitrogen source, which delivered a higher maximum power density (1122 mW/m^2) than Pt/C (988 mW/m^2) in MFCs. Similarly, Yang et al. prepared a N- and P-self-doped carbon catalyst using bamboo as the raw material, and the obtained catalyst achieved a performance (1056 ± 38 mW/m^2) similar to that of Pt/C (1039 ± 15 mW/m^2) in MFC. With $(NH_4)_3PO_4$ as the N and P source, a 65% increase in the maximum power density (1719 ± 82 mW/m^2) was obtained, compared to that without $(NH_4)_3PO_4$ modification (1056 ± 38 mW/m^2).[86] Some metal-based compounds have also been incorporated into biomass-derived carbon. Jing et al.[87] prepared N-doped carbon from cornstalk that was decorated with Fe_3Se_4/FeSe heterojunctions and found that the Fe_3Se_4/FeSe heterojunctions greatly promoted charge transfer and oxygen dissociation, and the N dopants in the carbon framework enhanced charge delocalization of the C atoms to reduce the electron loss, leading to enhanced electron utilization via a four-electron ($4e^-$) ORR pathway. However, it should be noted that the addition of heteroatom dopant precursors incurs additional preparation costs; thus, a balance must be struck between the enhancement of power output and the costs of heteroatom doping.

3.3. Assembly of Cathode Electrodes. The routing from ORR catalyst to cathode is a crucial step for practical applications. Typically, an air cathode consists of a catalyst layer (CL), a gas diffusion layer (GDL), and a support substrate. The design of the cathode architecture requires a porous CL allowing sufficient diffusion of oxygen and ions, a hydrophobic GDL to prevent the leakage of the electrolyte, and a high electrical conductivity support substrate for electron conduction. Most cathodes are fabricated by coating a layer of GDL on one side of the support substrate and a layer of CL on the other. For example, Cheng et al.[88] prepared an air cathode by following this two-step procedure: (i) preparation of GDL by coating four layers of a PTFE suspension onto one side of carbon cloth containing a carbon-based layer and heat treatment at 370 °C for 10 min and (ii) preparation of CL by coating one layer of a mixture of catalyst and binder onto the other side of the carbon cloth.

On the basis of the above cathode architecture and fabrication processes, it can be found that a critical step from catalyst to electrode is the fabrication of CL based on biomass-derived catalysts. During the CL preparation, different binders are used to avoid the detachment of catalysts from the cathode. For example, Wang et al.[89] prepared CL by first mixing a green foxtail-derived catalyst and a 5 wt % Nafion solution, then casting the mixture onto the electrode support substrate. However, the Nafion binder is too expensive for large-scale CL preparation needed for wastewater treatment. To decrease the cost of electrode fabrication, some other binders, such as PTFE, polyvinylidene fluoride (PVDF), and polydimethylsiloxane (PDMS), have been used as alternatives to Nafion, and partly hydrophobic CL using PTFE, PVDF, and PDMS as binders can facilitate oxygen transfer and three-phase interfaces (TPIs, with catalyst as the solid phase, electrolyte as the liquid phase, and oxygen as the gas phase) for ORR. For example, Bose et al.[90] prepared an air cathode by using sugar cane refuse-derived carbon as the catalyst and PVDF as the binder and prepared the CL by mixing the catalyst and PVDF and then casting the mixture onto a stainless steel mesh (SSM) substrate. Nevertheless, CLs are commonly prepared by brushing or dipping carbon cloth into the catalyst inks. The fabrication by brushing or dipping of PTFE, PVDF, or PDMS binder-based catalyst inks actually did not improve the performance of cathodes due to the poor TPIs. In addition, the brushing and dipping methods are rather crude and labor-intensive for commercialization.

https://dx.doi.org/10.1021/acs.iecr.0c00041
Ind. Eng. Chem. Res. 2020, 59, 6391−6404

To optimize the TPIs of CLs and develop an accurate and labor-saving method for CL fabrication, a rolling-press procedure has been proposed for cathode fabrication using biocarbon as the catalyst and SSM as the support substrate.[91] For example, Watson et al.[92,93] prepared an air cathode using biomass-derived (coconut shell, hardwood) activated carbon via the rolling-press procedure, by which a mixture of carbon black and PDMS and a mixture of the as-prepared catalyst and PTFE were rolled to be GDL and CL, respectively. The obtained GDL and CL were finally pressed onto the two sides of SSM to obtain the cathode. To further simplify the fabrication process, Yang et al.[94] presented a phase inversion process to prepare the cathode without the requirement of a heat-treatment, paste and press process. During the phase inversion process at room temperature, the PVDF diffuses out of the catalyst mixture and precipitates on the cathode surface to form a thin hydrophobic PVDF layer (Figure 9a), leading to

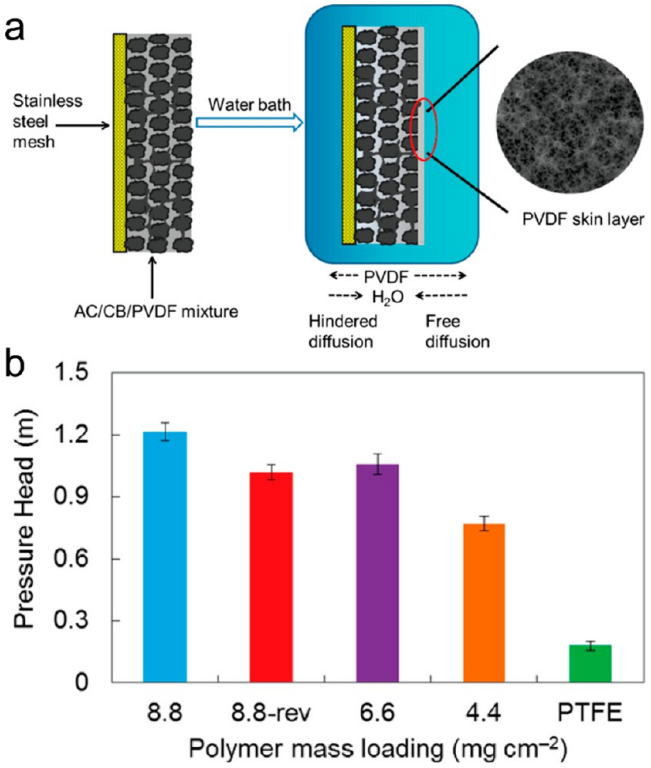

Figure 9. Schematic of cathode preparation based on phase inversion method. (b) Water pressure resistance of PVDF cathodes at different polymer loadings. Reprinted with permission from ref 94. Copyright 2014 American Chemical Society.

both binding of the catalyst onto the support substrate and formation of a polymer layer as the GDL. They found that the as-prepare cathode exhibited a satisfactory water pressure resistance of 1.22 ± 0.04 m without leakage (~12 kPa water head) (Figure 9b) and a power density of 1470 ± 50 mW/m^2 that was comparable to that of a Pt/C cathode. Note that in this simplified, accurate, and facile procedure for cathode fabrication, the usage of insulating binders might compromise the electrical conductivity of the cathode.

Binder-free cathodes are another promising option. Wang et al.[95] prepared a binder-free cathode by in situ growth of a nitrogen-doped graphene sheet on a nickel mesh as an efficient catalyst layer for MFC air cathodes, which delivered a maximum power density of 1470 ± 80 mW/m^2, 32% higher than that of a conventional Pt/C air cathode. However, this method is difficult to transplant to the cathode made by biomass-derived carbon. Yang et al.[96,97] prepared two kinds of monolithic binder-free cathodes using corrugated paper and bamboo tubes as the precursors. With the monolithic carbon structure derived from the precursors and heteroatom doping during pyrolysis, the obtained biocarbons served as ORR catalysts and support substrates simultaneously (Figure 10).

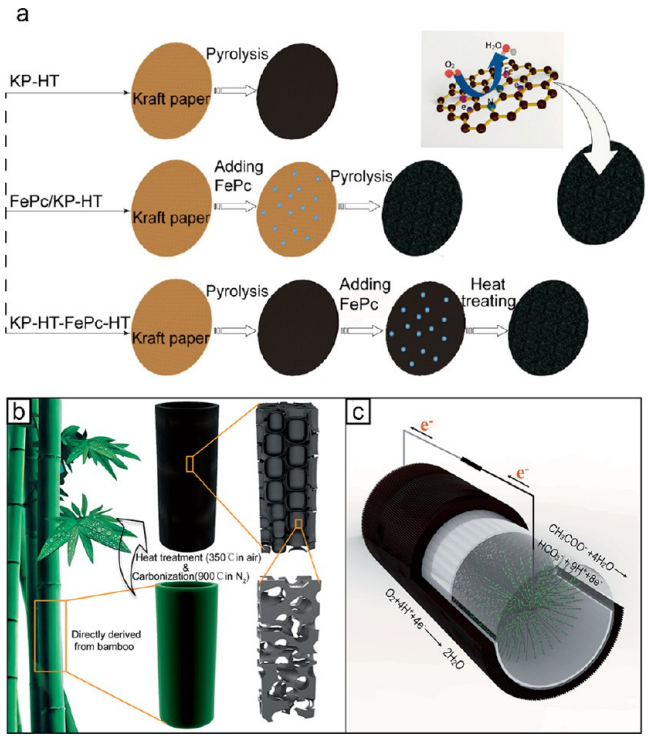

Figure 10. (a) Preparation procedure for corrugated paper-derived binder-free cathodes. Reprinted with permission from ref 96. Copyright 2017 Elsevier. (b, c) Schematic of bamboo tube-derived binder-free cathodes. Reprinted with permission from ref 97. Copyright 2017 Royal Society of Chemistry.

They found that both cathodes achieved a power output higher than that using the PTFE binder and also exhibited a high water pressure resistance (118 and 230 cm water pressure head, respectively). The concept of binder-free and monolithic fabrication can eliminate the need of a binder and support substrate, probably providing an alternative, effective avenue for air-cathode design.

3.4. Electrolyte−Electrode Interfacial Interaction. For a single-chamber air cathode MFC, CL is directly exposed to the electrolyte. Due to the high biocompatibility of biocarbon-based CL, microorganisms can be easily colonized on the CL surface and form a thick biofilm. The biofilm on the CL surface can function as a physical barrier against the diffusion of ions and oxygen, leading to an increasing concentration overpotential. In addition, the extracellular secretions of the biofilm may also change the physicochemical properties of CL and hence deteriorate the ORR activity. It has been shown that the formation of biofilm on the surface of activated carbon-based CL impedes the transport of hydroxide ions from the cathode to anode, and the pH near the CL surface can reach 11.6 ± 0.3 in the presence of a biofilm with an external load of 100 Ω, significantly higher than 9.4 ± 0.3 without a biofilm.[98] Several

https://dx.doi.org/10.1021/acs.iecr.0c00041
Ind. Eng. Chem. Res. 2020, 59, 6391−6404

approaches have been developed to inhibit biofilm formation on the surface of CLs, such as the addition of antibacterial reagents or nanoparticles in CLs and mechanical removal of biofilm.[99−103] For instance, Li et al.[102] modified the air cathode using a bifunctional quaternary ammonium compound by forced evaporation. They found that the modified cathode exhibited an apparent antibacterial performance and a low charge transfer resistance and a good cathode performance after 2 months of operation. Similarly, An et al.[101] prepared a cathode incorporated with silver nanoparticles, which delivered a lower protein mass (5.43 ± 0.016 g of protein mass/g of electrode) on the CL surface than the control cathode without silver nanoparticles (9.69 ± 0.095 g of protein mass/g of electrode), indicating effective biofilm inhibition. However, the modification using antibacterial reagents may block the pore structure of CL and cause secondary pollution of water, while the utilization of silver nanoparticles may increase the fabrication cost of the cathode.

In situ mechanical removal of biofilm and the incorporation of zinc oxides for biofilm inhibition have been employed to address these issues. For example, Rossi et al.[104] reported an in situ technique to remove biofilm on the cathode surface by placing a magnet on both sides of the electrode. When the air side of the magnet was moved, the magnet on the water side would scrap off the biofilm (Figure 11a). They found that the biomass content of the daily cleaned cathodes was 110 ± 29 $\mu g/cm^2$, which was 75% less than that of the control (441 ± 26 $\mu g/cm^2$) that was not cleaned daily after 1 month of operation. In spite of an immediate effect for biofilm removal, the method of mechanical cleaning may damage the CL, and the biofilm in the pores of CL still cannot be cleaned. Alternatively, Yang et al.[105] proposed a method to inhibit the formation of biofilm by using zinc oxide as an antibacterial reagent and porogen incorporated into the CL and observed that the as-prepared cathode in MFCs exhibited a more stable voltage output and power density than the Pt/C cathode. In addition, the surface of the as-prepared cathode had a biomass of 3.62 ± 1.74 mg/cm^2, which was much lower than that on the Pt/C cathode (11.41 ± 2.05 mg/cm^2) after 1 month of operation (Figure 11b). With these various strategies, whereas the amount of biomass is significantly reduced on the surface cathode, most studies of biofilm inhibition usually cover a span from 1 to 3 months, which is not sufficient to comprehensively evaluate the long-term stability of a cathode in practical applications. More prolonged studies are urgently needed.

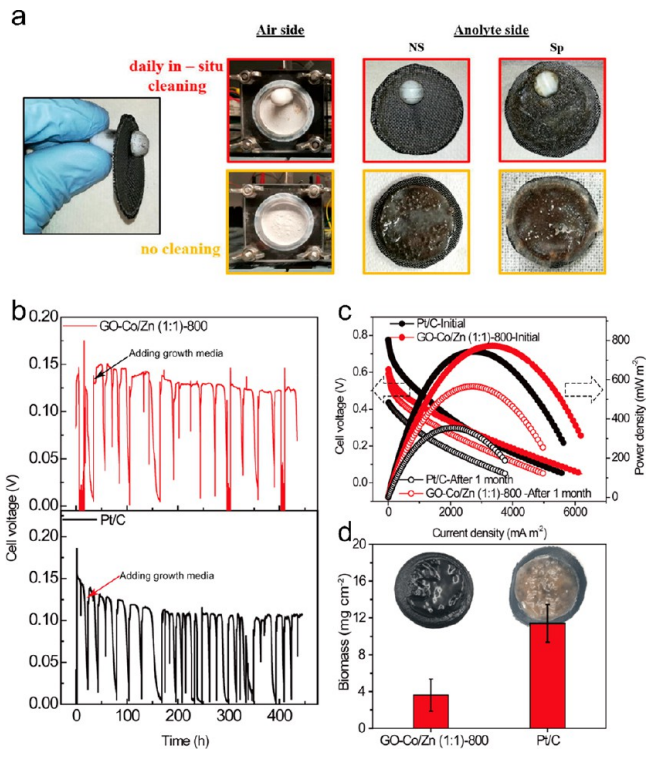

Figure 11. (a) Schematic of in situ removal of biofilm using a magnet. Reprinted with permission from ref 104. Copyright 2018 Elsevier. (b) Cell voltage. (c) Polarization and power density curves of MFCs using an antibacterial catalyst and Pt/C catalyst before and after 1 month of operation. (d) Biomass on the surfaces of cathodes after 1 month of operation. Panels (b−d) reprinted with permission from ref 105. Copyright 2019 Elsevier.

4. CONCLUSION AND PERSPECTIVES

MFC is a unique, new energy technology not only for sustainable energy conversion but also for wastewater treatment. Utilization of biomass-derived carbons as low-cost and high-performance MFC electrodes represents an important and attractive strategy. In this review, we summarize recent progress in the fabrication of electrodes based on biocarbon for MFC applications. One critical parameter is the electrode porosity, as the pore structure allows the colonization of bacteria on the internal surface and mass transport of substrate and ions in the interior of the anode. Meanwhile, a sufficient degree of heteroatom doping and high specific surface area is indispensable to increase the number and accessibility of the active sites, where architectural design of the cathode requires a feasible conversion from catalyst to electrode that facilitates electron transfer and mass transport of reaction intermediates and ions.

A variety of biomass from plants, animals, and sewage sludge have been exploited for electrode fabrication in MFC applications. Of these, the anodes made from select biomass, such as chestnut shell, loofah sponge, pomelo peel, and silk cocoon, exhibit a large pore distribution ranging from a few micrometers to several hundred micrometers, exhibiting a high anode performance and utilization rate. However, most other biomass-derived carbons exhibit a pore structure in the range of nanometers to a few micrometers, which cannot satisfy the requirement of microbial colonization, leading to a low utilization rate of the anode interior. As the anode porosity depends almost exclusively upon the choice of raw materials, exploring biomass precursors with pore sizes in the range of tens of micrometers to several hundreds of micrometers is crucial for the architecture design of the anode.

For cathode fabrication, a sufficiently high level of heteroatom doping is needed to achieve an adequate catalytic activity toward ORR. Some biomass, especially that from plants, exhibits a low nitrogen content of only 0.5−1.5 wt % in roots and stems and 3−5 wt % in leaves and a relatively low specific surface area;[46] in addition, there is an inevitable loss of part of the nitrogen during pyrolysis. Thus, additional heteroatom doping or an activation process is usually needed to improve the ORR activity. As the power density of MFCs is at least 2−3 orders of magnitude lower than that of chemical fuel cells, it is necessary to strike a good balance between increased preparation cost and improved power output through heteroatom doping or an activation process. Furthermore, cathode design involves a few functional layers

https://dx.doi.org/10.1021/acs.iecr.0c00041
Ind. Eng. Chem. Res. 2020, 59, 6391−6404

of CL, GDL, and support substrate. The commonly used methods for cathode preparation are based on the powder route, in which the biomass-derived carbon is first ground into a powder and then pasted onto the cathode substrate by mixing with a PTFE, PVDF, or PDMS binder. In spite of low costs and good oxygen diffusion, the involvement of binders in CL can decrease the electrical conductivity and wettability and therefore deteriorate the electron and ion transfer. These issues can be mitigated with the development of binder-free cathodes. Notably, binder-free cathodes are generally based on monolithic biocarbon, where the interconnected pores in the interior of the cathode can facilitate mass transport of oxygen and ions. Nevertheless, the excellent biocompatibility of biocarbon can induce the formation of biofilm on the surface of cathode. A variety of procedures have been described in the literature to inhibit biofilm growth, such as mechanical removal and chemical inhibition, which may damage the CL or cause secondary pollution of water. Also, the biofilm inhibition of the air cathode is typically evaluated within a period of 1−3 months, which is insufficient to fully address the issue of long-term stability in practical applications. Therefore, development of effective methods for biofilm inhibition remains critical to achieve stability in long-term operations.

Notably, a satisfactory electrochemical performance of the anode and/or cathode can, in general, be obtained, due to the unique features of biomass-derived electrodes: (i) increased electrode surface area for microbe loading and more active sites for ORR, (ii) abundant pores for mass transport of ions and oxygen, (iii) high electrical conductivity enabling fast electron transport and low resistance of the electrode, and (iv) low preparation cost that renders it possible for large-scale preparation of electrode materials and commercialization of MFCs. Nevertheless, it should be noted that research of MFCs is still in its infancy, and a range of critical challenges remain. In particular, the stability and longevity of biomass-derived electrodes has not been sufficiently examined in real wastewater, as most studies are conducted in artificial wastewater, and longevity tests are rarely reported. In addition, it is critical to attain repeatability of the biomass-derived carbon materials from different preparation batches, an important step toward commercialization of MFCs, since the biomass raw materials can impact the elemental composition, porosity, mechanical strength, and geometry structure of the eventual electrodes. Therefore, breakthroughs in these areas of research are highly desired in the advancement of the MFC technology in diverse applications, such as wastewater treatment, clean energy recovery, and biosensors.

■ ASSOCIATED CONTENT

Supporting Information

The Supporting Information is available free of charge at https://pubs.acs.org/doi/10.1021/acs.iecr.0c00041.

Information as mentioned in the text (PDF)

■ AUTHOR INFORMATION

Corresponding Authors

Wei Yang − *State Key Laboratory of Hydraulics and Mountain River Engineering, College of Water Resource & Hydropower, Sichuan University, Chengdu 610065, China*; Phone: +86-028-8540-5633; Email: wei_yang@scu.edu.cn

Shaowei Chen − *Department of Chemistry and Biochemistry, University of California, Santa Cruz, California 95064, United States*; orcid.org/0000-0002-3668-8551; Phone: 831-459-5841/831-459-2935; Email: shaowei@ucsc.edu

Complete contact information is available at: https://pubs.acs.org/10.1021/acs.iecr.0c00041

Author Contributions

The manuscript was written through contributions of all authors. All authors have given approval to the final version of the manuscript.

Notes

The authors declare no competing financial interest.

■ ACKNOWLEDGMENTS

This work was supported by the National Natural Science Foundation of China for Young Scientists (51906168 and 51606172, W.Y.) and the National Science Foundation (CHE-1900235 and CBET-1848841, S.W.C.).

■ REFERENCES

(1) Sindhuja, M.; Harinipriya, S.; Bala, A. C.; Ray, A. K. Environmentally available biowastes as substrate in microbial fuel cell for efficient chromium reduction. *J. Hazard. Mater.* **2018**, *355*, 197−205.

(2) Zhao, H. H.; Kong, C. H. Enhanced removal of p-nitrophenol in a microbial fuel cell after long-term operation and the catabolic versatility of its microbial community. *Chem. Eng. J.* **2018**, *339*, 424−431.

(3) Zhang, J.; Li, L. W.; Zheng, J. L.; Yang, P. L.; Wu, X. H.; Cheng, C. X.; Li, J.; Tian, Y. J.; Wang, F. Improved organic pollutants removal and simultaneous electricity production via integrating Fenton process and dual rotating disk photocatalytic fuel cell system using bamboo charcoal cathode. *Chem. Eng. J.* **2019**, *361*, 1198−1206.

(4) Bian, B.; Shi, D.; Cai, X. B.; Hu, M. J.; Guo, Q. Q.; Zhang, C. H.; Wang, Q.; Sun, A. X.; Yang, J. 3D printed porous carbon anode for enhanced power generation in microbial fuel cell. *Nano Energy* **2018**, *44*, 174−180.

(5) Liu, P. P.; Liang, P.; Jiang, Y.; Hao, W.; Miao, B.; Wang, D. L.; Huang, X. Stimulated electron transfer inside electroactive biofilm by magnetite for increased performance microbial fuel cell. *Appl. Energy* **2018**, *216*, 382−388.

(6) Mecheri, B.; Gokhale, R.; Santoro, C.; Costa de Oliveira, M. A.; D'Epifanio, A.; Licoccia, S.; Serov, A.; Artyushkova, K.; Atanassov, P. Oxygen Reduction Reaction Electrocatalysts Derived from Iron Salt and Benzimidazole and Aminobenzimidazole Precursors and Their Application in Microbial Fuel Cell Cathodes. *ACS. Appl. Energy Mater.* **2018**, *1* (10), 5755−5765.

(7) Song, R. B.; Wu, Y.; Lin, Z. Q.; Xie, J.; Tan, C. H.; Loo, J. S. C.; Cao, B.; Zhang, J. R.; Zhu, J. J.; Zhang, Q. Living and conducting: coating individual bacterial cells with in situ formed polypyrrole. *Angew. Chem., Int. Ed.* **2017**, *56* (35), 10516−10520.

(8) Yang, W.; Peng, Y.; Zhang, Y. D.; Lu, J. E.; Li, J.; Chen, S. W. Air Cathode Catalysts of Microbial Fuel Cell by Nitrogen-Doped Carbon Aerogels. *ACS Sustainable Chem. Eng.* **2019**, *7* (4), 3917−3924.

(9) Wang, Z. J.; Mahadevan, G. D.; Wu, Y. C.; Zhao, F. Progress of air-breathing cathode in microbial fuel cells. *J. Power Sources* **2017**, *356*, 245−255.

(10) Islam, M. A.; Ethiraj, B.; Cheng, C. K.; Yousuf, A.; Khan, M. M. R. An Insight of Synergy between Pseudomonas aeruginosa and Klebsiella variicola in a Microbial Fuel Cell. *ACS Sustainable Chem. Eng.* **2018**, *6* (3), 4130−4137.

(11) Li, J.; Hu, L.; Zhang, L.; Ye, D.-d.; Zhu, X.; Liao, Q. Uneven biofilm and current distribution in three-dimensional macroporous anodes of bio-electrochemical systems composed of graphite electrode arrays. *Bioresour. Technol.* **2017**, *228*, 25−30.

(12) Oliot, M.; Galier, S.; Roux de Balmann, H.; Bergel, A. Ion transport in microbial fuel cells: key roles, theory and critical review. *Appl. Energy* **2016**, *183*, 1682−1704.
(13) You, S.; Gong, X.; Wang, W.; Qi, D.; Wang, X.; Chen, X.; Ren, N. Enhanced Cathodic Oxygen Reduction and Power Production of Microbial Fuel Cell Based on Noble-Metal-Free Electrocatalyst Derived from Metal-Organic Frameworks. *Adv. Energy Mater.* **2016**, *6* (1), 1501497.
(14) Wang, R.; Yan, M.; Li, H.; Zhang, L.; Peng, B.; Sun, J.; Liu, D.; Liu, S. FeS_2 Nanoparticles Decorated Graphene as Microbial-Fuel-Cell Anode Achieving High Power Density. *Adv. Mater.* **2018**, *30*, 1800618.
(15) Zhao, C. E.; Gai, P. P.; Song, R. B.; Chen, Y.; Zhang, J. R.; Zhu, J. J. Nanostructured material-based biofuel cells: recent advances and future prospects. *Chem. Soc. Rev.* **2017**, *46* (5), 1545−1564.
(16) Song, R. B.; Zhu, W. L.; Fu, J. J.; Chen, Y.; Liu, L. X.; Zhang, J. R.; Lin, Y. H.; Zhu, J. J. Electrode Materials Engineering in Electrocatalytic CO2 Reduction: Energy Input and Conversion Efficiency. *Adv. Mater.* **2019**, 1903796.
(17) Pocaznoi, D.; Calmet, A.; Etcheverry, L.; Erable, B.; Bergel, A. Stainless steel is a promising electrode material for anodes of microbial fuel cells. *Energy Environ. Sci.* **2012**, *5* (11), 9645−9652.
(18) Baudler, A.; Schmidt, I.; Langner, M.; Greiner, A.; Schröder, U. Does it have to be carbon? Metal anodes in microbial fuel cells and related bioelectrochemical systems. *Energy Environ. Sci.* **2015**, *8* (7), 2048−2055.
(19) Karthikeyan, R.; Krishnaraj, N.; Selvam, A.; Wong, J. W. C.; Lee, P. K. H.; Leung, M. K. H.; Berchmans, S. Effect of composites based nickel foam anode in microbial fuel cell using Acetobacter aceti and Gluconobacter roseus as a biocatalysts. *Bioresour. Technol.* **2016**, *217*, 113−120.
(20) Chen, Y. M.; Wang, C. T.; Yang, Y. C.; Chen, W. J. Application of aluminum-alloy mesh composite carbon cloth for the design of anode/cathode electrodes in Escherichia coli microbial fuel cell. *Int. J. Hydrogen Energy* **2013**, *38* (25), 11131−11137.
(21) Jeong, C. M.; Choi, J. D. R.; Ahn, Y. H.; Chang, H. N. Removal of volatile fatty acids (VFA) by microbial fuel cell with aluminum electrode and microbial community identification with 16S rRNA sequence. *Korean J. Chem. Eng.* **2008**, *25* (3), 535−541.
(22) Zhou, X. W.; Chen, X. F.; Li, H. Y.; Xiong, J.; Li, X. P.; Li, W. S. Surface oxygen-rich titanium as anode for high performance microbial fuel cell. *Electrochim. Acta* **2016**, *209*, 582−590.
(23) Taskan, E.; Hasar, H. Comprehensive Comparison of a New Tin-Coated Copper Mesh and a Graphite Plate Electrode as an Anode Material in Microbial Fuel Cell. *Appl. Biochem. Biotechnol.* **2015**, *175* (4), 2300−2308.
(24) Li, S.; Cheng, C.; Thomas, A. Carbon-Based Microbial-Fuel-Cell Electrodes: From Conductive Supports to Active Catalysts. *Adv. Mater.* **2017**, *29* (8), 1602547.
(25) Xie, X.; Yu, G. H.; Liu, N.; Bao, Z. N.; Criddle, C. S.; Cui, Y. Graphene-sponges as high-performance low-cost anodes for microbial fuel cells. *Energy Environ. Sci.* **2012**, *5* (5), 6862−6866.
(26) Gnana Kumar, G.; Kirubaharan, C. J.; Udhayakumar, S.; Ramachandran, K.; Karthikeyan, C.; Renganathan, R.; Nahm, K. S. Synthesis, structural, and morphological characterizations of reduced graphene oxide-supported polypyrrole anode catalysts for improved microbial fuel cell performances. *ACS Sustainable Chem. Eng.* **2014**, *2* (10), 2283−2290.
(27) Zhao, C. E.; Wang, W. J.; Sun, D.; Wang, X.; Zhang, J. R.; Zhu, J. J. Nanostructured Graphene/TiO_2 Hybrids as High-Performance Anodes for Microbial Fuel Cells. *Chem. - Eur. J.* **2014**, *20* (23), 7091−7097.
(28) Ren, H.; Tian, H.; Gardner, C. L.; Ren, T. L.; Chae, J. A miniaturized microbial fuel cell with three-dimensional graphene macroporous scaffold anode demonstrating a record power density of over 10 000 W m^{-3}. *Nanoscale* **2016**, *8* (6), 3539−3547.
(29) Yang, Y.; Liu, T.; Zhu, X.; Zhang, F.; Ye, D.; Liao, Q.; Li, Y. Boosting Power Density of Microbial Fuel Cells with 3D Nitrogen-Doped Graphene Aerogel Electrode. *Adv. Sci.* **2016**, *3* (8), 1600097.
(30) Xie, X.; Ye, M.; Hu, L. B.; Liu, N.; McDonough, J. R.; Chen, W.; Alshareef, H. N.; Criddle, C. S.; Cui, Y. Carbon nanotube-coated macroporous sponge for microbial fuel cell electrodes. *Energy Environ. Sci.* **2012**, *5* (1), 5265−5270.
(31) Xie, X.; Hu, L.; Pasta, M.; Wells, G. F.; Kong, D.; Criddle, C. S.; Cui, Y. Three-dimensional carbon nanotube-textile anode for high-performance microbial fuel cells. *Nano Lett.* **2011**, *11* (1), 291−296.
(32) Mink, J. E.; Rojas, J. P.; Logan, B. E.; Hussain, M. M. Vertically Grown Multiwalled Carbon Nanotube Anode and Nickel Silicide Integrated High Performance Microsized (1.25 μL) Microbial Fuel Cell. *Nano Lett.* **2012**, *12* (2), 791−795.
(33) Mink, J. E.; Hussain, M. M. Sustainable Design of High-Performance Microsized Microbial Fuel Cell with Carbon Nanotube Anode and Air Cathode. *ACS Nano* **2013**, *7* (8), 6921−6927.
(34) Zhao, Y.; Watanabe, K.; Nakamura, R.; Mori, S.; Liu, H.; Ishii, K.; Hashimoto, K. Three-Dimensional Conductive Nanowire Networks for Maximizing Anode Performance in Microbial Fuel Cells. *Chem. - Eur. J.* **2010**, *16* (17), 4982−4985.
(35) Sonawane, J. M.; Yadav, A.; Ghosh, P. C.; Adeloju, S. B. Recent advances in the development and utilization of modern anode materials for high performance microbial fuel cells. *Biosens. Bioelectron.* **2017**, *90*, 558−576.
(36) Wang, H. Y.; Wang, G. M.; Ling, Y. C.; Qian, F.; Song, Y.; Lu, X. H.; Chen, S. W.; Tong, Y. X.; Li, Y. High power density microbial fuel cell with flexible 3D graphene-nickel foam as anode. *Nanoscale* **2013**, *5* (21), 10283−10290.
(37) Jang, S.; Kim, S.; Kim, S. M.; Choi, J.; Yeon, J.; Bang, K.; Ahn, C. Y.; Hwang, W.; Her, M.; Cho, Y. H.; Sung, Y. E.; Choi, M. Interface engineering for high-performance direct methanol fuel cells using multiscale patterned membranes and guided metal cracked layers. *Nano Energy* **2018**, *43*, 149−158.
(38) Li, Y. X.; Liang, L.; Liu, C. P.; Li, Y.; Xing, W.; Sun, J. Q. Self-Healing Proton-Exchange Membranes Composed of Nafion-Poly-(vinyl alcohol) Complexes for Durable Direct Methanol Fuel Cells. *Adv. Mater.* **2018**, *30* (25), 1707146.
(39) Li, Y. S.; Feng, Y.; Sun, X. D.; He, Y. L. A Sodium-Ion-Conducting Direct Formate Fuel Cell: Generating Electricity and Producing Base. *Angew. Chem., Int. Ed.* **2017**, *56* (21), 5734−5737.
(40) Li, Y. S.; Sun, X. D.; Feng, Y. Hydroxide Self-Feeding High-Temperature Alkaline Direct Formate Fuel Cells. *ChemSusChem* **2017**, *10* (10), 2135−2139.
(41) Zamani, P.; Higgins, D. C.; Hassan, F. M.; Fu, X. G.; Choi, J. Y.; Hoque, M. A.; Jiang, G. P.; Chen, Z. W. Highly active and porous graphene encapsulating carbon nanotubes as a non-precious oxygen reduction electrocatalyst for hydrogen-air fuel cells. *Nano Energy* **2016**, *26*, 267−275.
(42) Wang, H. M.; Park, J. D.; Ren, Z. J. Practical Energy Harvesting for Microbial Fuel Cells: A Review. *Environ. Sci. Technol.* **2015**, *49* (6), 3267−3277.
(43) Zhang, L. J.; He, W. H.; Yang, J. C.; Sun, J. Q.; Li, H. D.; Han, B.; Zhao, S. L.; Shi, Y. A.; Feng, Y. J.; Tang, Z. Y.; Liu, S. Q. Bread-derived 3D macroporous carbon foams as high performance free-standing anode in microbial fuel cells. *Biosens. Bioelectron.* **2018**, *122*, 217−223.
(44) Chen, Q.; Pu, W. H.; Hou, H. J.; Hu, J. P.; Liu, B. C.; Li, J. F.; Cheng, K.; Huang, L.; Yuan, X. Q.; Yang, C. Z.; Yang, J. K. Activated microporous-mesoporous carbon derived from chestnut shell as a sustainable anode material for high performance microbial fuel cells. *Bioresour. Technol.* **2018**, *249*, 567−573.
(45) Yuan, H. R.; Dong, G.; Li, D. N. A.; Deng, L. F.; Cheng, P.; Chen, Y. Steamed cake-derived 3D carbon foam with surface anchored carbon nanoparticles as freestanding anodes for high-performance microbial fuel cells. *Sci. Total Environ.* **2018**, *636*, 1081−1088.
(46) Antolini, E. Nitrogen-doped carbons by sustainable N-and C-containing natural resources as nonprecious catalysts and catalyst supports for low temperature fuel cells. *Renewable Sustainable Energy Rev.* **2016**, *58*, 34−51.

https://dx.doi.org/10.1021/acs.iecr.0c00041
Ind. Eng. Chem. Res. 2020, 59, 6391−6404

(47) Chen, S. S.; Tang, J. H.; Jing, X. Y.; Liu, Y.; Yuan, Y.; Zhou, S. G. A hierarchically structured urchin-like anode derived from chestnut shells for microbial energy harvesting. *Electrochim. Acta* **2016**, *212*, 883−889.
(48) Zhu, H. L.; Wang, H. M.; Li, Y. Y.; Bao, W. Z.; Fang, Z. Q.; Preston, C.; Vaaland, O.; Ren, Z. Y.; Hu, L. B. Lightweight, conductive hollow fibers from nature as sustainable electrode materials for microbial energy harvesting. *Nano Energy* **2014**, *10*, 268−276.
(49) Xie, X.; Hu, L.; Pasta, M.; Wells, G. F.; Kong, D.; Criddle, C. S.; Cui, Y. Three-dimensional carbon nanotube-textile anode for high-performance microbial fuel cells. *Nano Lett.* **2011**, *11* (1), 291−296.
(50) Zhou, L. H.; Sun, L. H.; Fu, P.; Yang, C. L.; Yuan, Y. Carbon nanoparticles of Chinese ink-wrapped natural loofah sponge: a low-cost three-dimensional electrode for high-performance microbial energy harvesting. *J. Mater. Chem. A* **2017**, *5* (28), 14741−14747.
(51) Zheng, J. L.; Cheng, C. X.; Zhang, J.; Wu, X. H. Appropriate mechanical strength of carbon black-decorated loofah sponge as anode material in microbial fuel cells. *Int. J. Hydrogen Energy* **2016**, *41* (48), 23156−23163.
(52) Lu, M.; Qian, Y.; Yang, C.; Huang, X.; Li, H.; Xie, X.; Huang, L.; Huang, W. Nitrogen-enriched pseudographitic anode derived from silk cocoon with tunable flexibility for microbial fuel cells. *Nano Energy* **2017**, *32*, 382−388.
(53) Feng, H. J.; Jia, Y. F.; Shen, D. S.; Zhou, Y. Y.; Chen, T.; Chen, W.; Ge, Z. P.; Zheng, S. T.; Wang, M. Z. The effect of chemical vapor deposition temperature on the performance of binder-free sewage sludge-derived anodes in microbial fuel cells. *Sci. Total Environ.* **2018**, *635*, 45−52.
(54) Jia, Y. F.; Feng, H. J.; Shen, D. S.; Zhou, Y. Y.; Chen, T.; Wang, M. Z.; Chen, W.; Ge, Z. P.; Huang, L. J.; Zheng, S. T. High-performance microbial fuel cell anodes obtained from sewage sludge mixed with fly ash. *J. Hazard. Mater.* **2018**, *354*, 27−32.
(55) Yuan, Y.; Liu, T.; Fu, P.; Tang, J.; Zhou, S. Conversion of sewage sludge into high-performance bifunctional electrode materials for microbial energy harvesting. *J. Mater. Chem. A* **2015**, *3* (16), 8475−8482.
(56) Speers, A. M.; Reguera, G. Electron Donors Supporting Growth and Electroactivity of Geobacter sulfurreducens Anode Biofilms. *Appl. Environ. Microbiol.* **2012**, *78* (2), 437−444.
(57) Korth, B.; Rosa, L. F. M.; Harnisch, F.; Picioreanu, C. A framework for modeling electroactive microbial biofilms performing direct electron transfer. *Bioelectrochemistry* **2015**, *106*, 194−206.
(58) Goller, C. C.; Romeo, T. Environmental influences on biofilm development. *Curr. Top. Microbiol. Immunol.* **2008**, *322*, 37−66.
(59) Yazdi, A. A.; D'Angelo, L.; Omer, N.; Windiasti, G.; Lu, X. N.; Xu, J. Carbon nanotube modification of microbial fuel cell electrodes. *Biosens. Bioelectron.* **2016**, *85*, 536−552.
(60) Hindatu, Y.; Annuar, M.; Gumel, A. Mini-review: Anode modification for improved performance of microbial fuel cell. *Renewable Sustainable Energy Rev.* **2017**, *73*, 236−248.
(61) Wang, R. W.; Liu, D.; Yan, M.; Zhang, L.; Chang, W.; Sun, Z. Y.; Liu, S. Q.; Guo, C. S. Three-dimensional high performance free-standing anode by one-step carbonization of pinecone in microbial fuel cells. *Bioresour. Technol.* **2019**, *292*, 121956.
(62) Zhang, J.; Li, J.; Ye, D.; Zhu, X.; Liao, Q.; Zhang, B. Tubular bamboo charcoal for anode in microbial fuel cells. *J. Power Sources* **2014**, *272*, 277−282.
(63) Zhang, L.; Zhu, X.; Li, J.; Liao, Q.; Ye, D. Biofilm formation and electricity generation of a microbial fuel cell started up under different external resistances. *J. Power Sources* **2011**, *196* (15), 6029−6035.
(64) Li, J.; Li, H. J.; Zheng, J. L.; Zhang, L.; Fu, Q.; Zhu, X.; Liao, Q. Response of anodic biofilm and the performance of microbial fuel cells to different discharging current densities. *Bioresour. Technol.* **2017**, *233*, 1−6.
(65) Zhang, E. R.; Xu, W.; Diao, G. W.; Shuang, C. D. Electricity generation from acetate and glucose by sedimentary bacterium attached to electrode in microbial-anode fuel cells. *J. Power Sources* **2006**, *161* (2), 820−825.
(66) Chong, P.; Erable, B.; Bergel, A. Effect of pore size on the current produced by 3-dimensional porous microbial anodes: A critical review. *Bioresour. Technol.* **2019**, *289*, 121641.
(67) Karthikeyan, R.; Wang, B.; Xuan, J.; Wong, J. W.; Lee, P. K.; Leung, M. K. Interfacial electron transfer and bioelectrocatalysis of carbonized plant material as effective anode of microbial fuel cell. *Electrochim. Acta* **2015**, *157*, 314−323.
(68) Chen, S.; He, G.; Hu, X.; Xie, M.; Wang, S.; Zeng, D.; Hou, H.; Schröder, U. A three-dimensionally ordered macroporous carbon derived from a natural resource as anode for microbial bioelectrochemical systems. *ChemSusChem* **2012**, *5* (6), 1059−1063.
(69) Chen, S.; Liu, Q.; He, G.; Zhou, Y.; Hanif, M.; Peng, X.; Wang, S.; Hou, H. Reticulated carbon foam derived from a sponge-like natural product as a high-performance anode in microbial fuel cells. *J. Mater. Chem.* **2012**, *22* (35), 18609−18613.
(70) Chen, S. L.; He, G. H.; Liu, Q.; Harnisch, F.; Zhou, Y.; Chen, Y.; Hanif, M.; Wang, S. Q.; Peng, X. W.; Hou, H. Q.; Schroder, U. Layered corrugated electrode macrostructures boost microbial bioelectrocatalysis. *Energy Environ. Sci.* **2012**, *5* (12), 9769−9772.
(71) Flexer, V.; Donose, B. C.; Lefebvre, C.; Pozo, G.; Boone, M. N.; Van Hoorebeke, L.; Baccour, M.; Bonnet, L.; Calas-Etienne, S.; Galarneau, A.; Titirici, M. M.; Brun, N. Microcellular Electrode Material for Microbial Bioelectrochemical Systems Synthesized by Hydrothermal Carbonization of Biomass Derived Precursors. *ACS Sustainable Chem. Eng.* **2016**, *4* (5), 2508−2516.
(72) Li, J.; Zhang, J.; Ye, D. D.; Zhu, X.; Liao, Q.; Zheng, J. L. Optimization of inner diameter of tubular bamboo charcoal anode for a microbial fuel cell. *Int. J. Hydrogen Energy* **2014**, *39* (33), 19242−19248.
(73) He, Z. M.; Liu, J.; Qiao, Y.; Li, C. M.; Tan, T. T. Y. Architecture Engineering of Hierarchically Porous Chitosan/Vacuum-Stripped Graphene Scaffold as Bioanode for High Performance Microbial Fuel Cell. *Nano Lett.* **2012**, *12* (9), 4738−4741.
(74) Zhong, K. Q.; Li, M.; Yang, Y.; Zhang, H. G.; Zhang, B. P.; Tang, J. F.; Yan, J.; Su, M. H.; Yang, Z. Q. Nitrogen-doped biochar derived from watermelon rind as oxygen reduction catalyst in air cathode microbial fuel cells. *Appl. Energy* **2019**, *242*, 516−525.
(75) Fan, Z.; Li, J.; Zhou, Y.; Fu, Q.; Yang, W.; Zhu, X.; Liao, Q. A green, cheap, high-performance carbonaceous catalyst derived from Chlorella pyrenoidosa for oxygen reduction reaction in microbial fuel cells. *Int. J. Hydrogen Energy* **2017**, *42* (45), 27657−27665.
(76) Zhou, L.; Fu, P.; Cai, X.; Zhou, S.; Yuan, Y. Naturally derived carbon nanofibers as sustainable electrocatalysts for microbial energy harvesting: A new application of spider silk. *Appl. Catal., B* **2016**, *188*, 31−38.
(77) Yuan, H. R.; Deng, L. F.; Cai, X. X.; Zhou, S. G.; Chen, Y.; Yuan, Y. Nitrogen-doped carbon sheets derived from chitin as non-metal bifunctional electrocatalysts for oxygen reduction and evolution. *RSC Adv.* **2015**, *5* (69), 56121−56129.
(78) Deng, L.; Yuan, H.; Cai, X.; Ruan, Y.; Zhou, S.; Chen, Y.; Yuan, Y. Honeycomb-like hierarchical carbon derived from livestock sewage sludge as oxygen reduction reaction catalysts in microbial fuel cells. *Int. J. Hydrogen Energy* **2016**, *41* (47), 22328−22336.
(79) Li, M.; Zhang, H. G.; Xiao, T. F.; Wang, S. D.; Zhang, B. P.; Chen, D. Y.; Su, M. H.; Tang, J. F. Low-cost biochar derived from corncob as oxygen reduction catalyst in air cathode microbial fuel cells. *Electrochim. Acta* **2018**, *283*, 780−788.
(80) Zhu, C.; Zhai, J.; Dong, S. Bifunctional fluorescent carbon nanodots: green synthesis via soy milk and application as metal-free electrocatalysts for oxygen reduction. *Chem. Commun.* **2012**, *48* (75), 9367−9369.
(81) Zhou, L.; Fu, P.; Wen, D.; Yuan, Y.; Zhou, S. Self-constructed carbon nanoparticles-coated porous biocarbon from plant moss as advanced oxygen reduction catalysts. *Appl. Catal., B* **2016**, *181*, 635−643.
(82) Li, D.; Deng, L.; Yuan, H.; Dong, G.; Chen, J.; Zhang, X.; Chen, Y.; Yuan, Y. N, P-doped mesoporous carbon from onion as

https://dx.doi.org/10.1021/acs.iecr.0c00041
Ind. Eng. Chem. Res. 2020, 59, 6391−6404

trifunctional metal-free electrode modifier for enhanced power performance and capacitive manner of microbial fuel cells. *Electrochim. Acta* **2018**, *262*, 297−305.
(83) Ye, W. Y.; Tang, J. H.; Wang, Y. J.; Cai, X. X.; Liu, H. W.; Lin, J. Y.; Van der Bruggen, B.; Zhou, S. G. Hierarchically structured carbon materials derived from lotus leaves as efficient electrocatalyst for microbial energy harvesting. *Sci. Total Environ.* **2019**, *666*, 865−874.
(84) Deng, L.; Yuan, Y.; Zhang, Y.; Wang, Y.; Chen, Y.; Yuan, H.; Chen, Y. Alfalfa leaf-derived porous heteroatom-doped carbon materials as efficient cathodic catalysts in microbial fuel cells. *ACS Sustainable Chem. Eng.* **2017**, *5* (11), 9766−9773.
(85) Sun, Y.; Duan, Y. Q.; Hao, L.; Xing, Z. P.; Dai, Y.; Li, R.; Zou, J. L. Cornstalk-Derived Nitrogen-Doped Partly Graphitized Carbon as Efficient Metal-Free Catalyst for Oxygen Reduction Reaction in Microbial Fuel Cells. *ACS Appl. Mater. Interfaces* **2016**, *8* (39), 25923−25932.
(86) Yang, W.; Li, J.; Ye, D.; Zhu, X.; Liao, Q. Bamboo charcoal as a cost-effective catalyst for an air-cathode of microbial fuel cells. *Electrochim. Acta* **2017**, *224*, 585−592.
(87) Jing, B. J.; You, S. J.; Ma, Y. Y.; Xing, Z. P.; Chen, H.; Dai, Y.; Zhang, C. Y.; Ren, N. Q.; Zou, J. L. Fe3Se4/FeSe heterojunctions in cornstalk-derived N-doped carbon framework enhance charge transfer and cathodic oxygen reduction reaction to boost bio-electricity generation. *Appl. Catal., B* **2019**, *244*, 465−474.
(88) Cheng, S.; Liu, H.; Logan, B. E. Increased performance of single-chamber microbial fuel cells using an improved cathode structure. *Electrochem. Commun.* **2006**, *8* (3), 489−494.
(89) Wang, X. H.; Gong, X. B.; Peng, L.; Yang, Z.; Liu, Y. Tubular nitrogen-doped carbon materials derived from green foxtail as a metal-free electrocatalyst in microbial fuel cells for efficient electron generation. *Bioelectrochemistry* **2019**, *127*, 104−112.
(90) Bose, D.; Sridharan, S.; Dhawan, H.; Vijay, P.; Gopinath, M. Biomass derived activated carbon cathode performance for sustainable power generation from Microbial Fuel Cells. *Fuel* **2019**, *236*, 325−337.
(91) Dong, H.; Yu, H.; Wang, X.; Zhou, Q.; Feng, J. A novel structure of scalable air-cathode without Nafion and Pt by rolling activated carbon and PTFE as catalyst layer in microbial fuel cells. *Water Res.* **2012**, *46* (17), 5777−5787.
(92) Watson, V. J.; Nieto Delgado, C.; Logan, B. E. Improvement of activated carbons as oxygen reduction catalysts in neutral solutions by ammonia gas treatment and their performance in microbial fuel cells. *J. Power Sources* **2013**, *242*, 756−761.
(93) Watson, V. J.; Nieto Delgado, C.; Logan, B. E. Influence of chemical and physical properties of activated carbon powders on oxygen reduction and microbial fuel cell performance. *Environ. Sci. Technol.* **2013**, *47* (12), 6704−6710.
(94) Yang, W.; He, W.; Zhang, F.; Hickner, M. A.; Logan, B. E. Single-step fabrication using a phase inversion method of poly (vinylidene fluoride)(PVDF) activated carbon air cathodes for microbial fuel cells. *Environ. Sci. Technol. Lett.* **2014**, *1* (10), 416−420.
(95) Wang, Q.; Zhang, X.; Lv, R.; Chen, X.; Xue, B.; Liang, P.; Huang, X. Binder-free nitrogen-doped graphene catalyst air-cathodes for microbial fuel cells. *J. Mater. Chem. A* **2016**, *4* (32), 12387−12391.
(96) Yang, W.; Li, J.; Fu, Q.; Zhang, L.; Zhu, X.; Liao, Q. A simple method for preparing a binder-free paper-based air cathode for microbial fuel cells. *Bioresour. Technol.* **2017**, *241*, 325−331.
(97) Yang, W.; Li, J.; Zhang, L.; Zhu, X.; Liao, Q. A monolithic air cathode derived from bamboo for microbial fuel cells. *RSC Adv.* **2017**, *7* (45), 28469−28475.
(98) Yuan, Y.; Zhou, S.; Tang, J. In situ investigation of cathode and local biofilm microenvironments reveals important roles of OH−and oxygen transport in microbial fuel cells. *Environ. Sci. Technol.* **2013**, *47* (9), 4911−4917.
(99) Li, D.; Qu, Y.; Liu, J.; Liu, G.; Zhang, J.; Feng, Y. Enhanced oxygen and hydroxide transport in a cathode interface by efficient antibacterial property of a silver nanoparticle-modified, activated carbon cathode in microbial fuel cells. *ACS Appl. Mater. Interfaces* **2016**, *8* (32), 20814−20821.
(100) Amin, M. A.; Fadlallah, S. A.; Alosaimi, G. S. In situ aqueous synthesis of silver nanoparticles supported on titanium as active electrocatalyst for the hydrogen evolution reaction. *Int. J. Hydrogen Energy* **2014**, *39* (34), 19519−19540.
(101) An, J.; Jeon, H.; Lee, J.; Chang, I. S. Bifunctional silver nanoparticle cathode in microbial fuel cells for microbial growth inhibition with comparable oxygen reduction reaction activity. *Environ. Sci. Technol.* **2011**, *45* (12), 5441−5446.
(102) Li, N.; Liu, Y.; An, J.; Feng, C.; Wang, X. Bifunctional quaternary ammonium compounds to inhibit biofilm growth and enhance performance for activated carbon air-cathode in microbial fuel cells. *J. Power Sources* **2014**, *272*, 895−899.
(103) Liu, W.; Cheng, S.; Sun, D.; Huang, H.; Chen, J.; Cen, K. Inhibition of microbial growth on air cathodes of single chamber microbial fuel cells by incorporating enrofloxacin into the catalyst layer. *Biosens. Bioelectron.* **2015**, *72*, 44−50.
(104) Rossi, R.; Yang, W. L.; Zikmund, E.; Pant, D.; Logan, B. E. In situ biofilm removal from air cathodes in microbial fuel cells treating domestic wastewater. *Bioresour. Technol.* **2018**, *265*, 200−206.
(105) Yang, W.; Chata, G.; Zhang, Y. D.; Peng, Y.; Lu, J. E.; Wang, N.; Mercado, R.; Li, J.; Chen, S. W. Graphene oxide-supported zinc cobalt oxides as effective cathode catalysts for microbial fuel cell: High catalytic activity and inhibition of biofilm formation. *Nano Energy* **2019**, *57*, 811−819.

https://dx.doi.org/10.1021/acs.iecr.0c00041
Ind. Eng. Chem. Res. 2020, 59, 6391−6404